COMMUNICATION

Check for updates

Visualizing back electron transfer in eosin Y photoredox catalysis†

Kai Gu,[a] Wenqiao Zhou[a] and Chunming Liu ⓘ *[ab]

Back electron transfer (BET) in eosin Y (EY) photoredox catalysis was visualized *via* the fluorescence of single EYs. BET between the radical ion pair formed in photoinduced electron transfer (PET) induced photoblinking of single EYs under constant photoexcitation. Commonly used quenchers, alkyl bromides and a tertiary amine, were studied. BET was observed in alkyl bromides, but not in the tertiary amine. The findings helped explain the mechanism of EY-catalyzed photoinduced atom transfer radical polymerizations. The method can be applied to studying BET on photo-emissive catalysts.

Photoredox catalysis has been widely used for organic synthesis in the past decade.[1–9] The field has been growing rapidly due to the unique advantages of photoredox catalysis, *e.g.*, mild reaction conditions, high energy efficiency, and the ease of controlling the process by light illumination. The photoredox catalyst (PC) is the essential component that absorbs light energy and initiates the photocatalytic cycle. In the electron-transfer mechanism, a radical ion pair, $PC^{\bullet+}–Q^{\bullet-}$ (or $PC^{\bullet-}–Q^{\bullet+}$), is formed *via* photoinduced electron transfer and is expected to be embedded in a solvent cage (Fig. 1a).[10–12] The radical ion pair could recombine to return to ground state molecules, which is referred to as back electron transfer (BET) or charge recombination (Fig. 1a).[10–12] BET is thermodynamically favored and would make the product formation slower, because the radical ions are consumed without producing final products.[13–15] In some reactions, BET could also be the key step to get the desired product. For example, in photocatalytic controlled radical polymerizations, the reversible deactivation of polymer growth is achieved through the BET between the PC radical and the propagating radical that are generated *via* photoinduced electron transfer (PET).[16–18] Currently, BET is studied experimentally by comparing the concentration of the

photoproduct after pulsed excitation of a sample with that of a reference solution that is expected to have a known BET yield.[19–21] However, the direct observation of the BET process is difficult to achieve.

In this work, we demonstrate the direct visualization of BET by single-molecule fluorescence imaging. Previously, we developed the single-molecule fluorescence imaging method to study photoredox catalysis in operando, in which the redox states of individual PCs were monitored *via* their fluorescence signal.[22] Continuous photocatalytic turnovers give rise to the reversible switching of single PC's redox states, and result in the photoblinking behavior of single PCs under continuous photoexcitation. Here, we will monitor the behavior of single PCs in the solutions of a single quencher. If BET does not occur between the quencher radical ion ($Q^{\bullet+}$ or $Q^{\bullet-}$) and PC radical ion ($PC^{\bullet-}$ or $PC^{\bullet+}$), the fluorescence of individual EYs should be quenched in a single step due to the photoinduced electron transfer (Fig. 1b). If BET occurs, the PC radical ion ($PC^{\bullet-}$ or $PC^{\bullet+}$) could
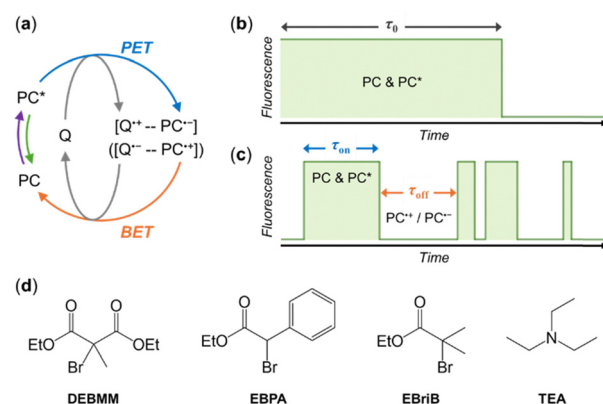

Fig. 1 (a) The diagram of photoinduced electron transfer (PET) and back electron transfer (BET) in electron-transfer photoredox catalysis. Q: quencher; PC: photoredox catalyst; PC*: photoexcited PC. The rectangular brackets represent the solvent cage. (b) and (c) Expected behavior of a single photoredox catalyst (PC) in the quencher (b) without BET and (c) with BET. (d) The chemical structures of the quenchers used in this work.

[a] *School of Polymer Science and Polymer Engineering, University of Akron, Akron, OH, 44325, USA. E-mail: chunmingliu@uakron.edu*

[b] *Department of Chemistry, University of Akron, Akron, OH, 44325, USA*

† Electronic supplementary information (ESI) available. See DOI: https://doi.org/10.1039/d4cc04463k

return to ground state PC, and the fluorescence of the PC would be restored, giving rise to the photoblinking of PC (Fig. 1c). Besides, energy transfer between PC* and the quencher cannot change the redox state of PC, and therefore no additional photoblinking of PC should be observed if the quenching follows the energy transfer mechanism.

We monitored the behavior of single eosin Y (EY) in commonly used quenchers (Fig. 1d), including three alkyl bromides, diethyl 2-bromo-2-methylmalonate (DEBMM), ethyl α-bromophenylacetate (EBPA) and methyl α-bromoisobutyrate (MBriB), and a tertiary amine, triethylamine (TEA). EY is a commonly used photoredox catalyst that absorbs green light.[6,23] Alkyl bromides are expected to quench EY via oxidative quenching, while tertiary amine is expected to quench EY via reductive quenching.[23] Single-molecule imaging of EYs was carried out following the procedure we reported previously (Section S1, ESI†).[22,24] Briefly, DMF was used as the solvent for all experiments, and the solutions were degassed and protected under N_2 during imaging. EYs were immobilized on the glass surface and imaged using total-internal reflection fluorescence microscope. The fluorescence trajectories of individual EYs were analyzed using the MATLAB program.[22,25]

In DEBMM, both single-step photobleaching and photo-blinking of single EYs were observed (Fig. 2a). This suggested the existence of the process that makes the EY radical ion ($EY^{\bullet+}$) return to the ground state. Since no other reactants were present in the solution besides DEBMM, the BET between

$EY^{\bullet+}$ and the DEBMM radical anion ($DEBMM^{\bullet-}$) should be responsible for the photoblinking of single EYs' fluorescence (Fig. 1c). The photobleaching of EYs was accelerated by DEBMM and the photobleaching time τ_0 (defined as shown in Fig. 1b) became shorter with increasing DEBMM concentration. The photobleaching rate of EY (T_0^{-1}), calculated by the inverse of the decay constant of τ_0 (Fig. S1 and section S2, ESI†), was linearly correlated to the concentration of DEBMM (Fig. 2b). It was consistent with the Stern–Volmer quenching results that DEBMM effectively quenched EY.[26]

The percentage of photoblinking EY (P_{blink}) increased with DEBMM concentration (Fig. 2c). On the one hand, the increase of P_{blink} was due to the more efficient quenching of EY at higher DEBMM concentration, which is the prerequisite to generate photoblinking. On the other hand, the increase of P_{blink} also indicated that BET between $EY^{\bullet+}$ and $DEBMM^{\bullet-}$ was efficient. The distributions of fluorescence on-time τ_{on} and off-time τ_{off} of photoblinking EYs (as defined in Fig. 1c) were also investigated. τ_{on} followed double-exponential distribution (Fig. S2, ESI†), and τ_{off} followed single-exponential distribution (Fig. S3, ESI†), which are consistent with our previous results.[22] T_{on1}, the faster decay constant of τ_{on}, did not show an obvious change with DEBMM concentration, indicating that the faster quenching of EY* reached saturation in the DEBMM concentration range (Fig. 2d). T_{on2}, the slower decay constant of τ_{on}, decreased with DEBMM concentration (Fig. 2d), which further supported that DEBMM was responsible for the quenching of EY. On the other hand, T_{off}, the decay constant of τ_{off}, was independent of DEBMM concentration (Fig. 2e). Based on our interpretation, T_{off}^{-1} should represent the BET rate. Recently, it was reported that the BET rate is independent of quencher concentration.[19] This result supported our hypothesis that BET between the radical ion pair ($EY^{\bullet+}$ and $DEBMM^{\bullet-}$) induced the photoblinking of EYs.

Next, we studied the effect of alkyl bromide structure on the behavior of single EYs. Two other alkyl bromides, EBPA and MBriB, were investigated, and gave similar results as DEBMM. Both EBPA and MBriB induced photoblinking of EYs indicating that BET occurred between $EY^{\bullet+}$ and radical anions of EBPA and MBriB. Similarly, the photobleaching rate of EY (T_0^{-1}) by EBPA and MBriB was linearly correlated with their concentration, respectively (Fig. 3a).

Compared to DEBMM, EBPA induced higher percentages of photoblinking EY at lower concentrations (Fig. 3b) and gave faster photobleaching of EY (Fig. 3a). In contrast, MBriB induced lower percentages of photoblinking EY at even higher concentrations (Fig. 3b) and gave slower photobleaching of EY (Fig. 3a). The differences could be due to the structures of DEBMM, EBPA and MBriB and the properties of their anion radicals.[27] The EBPA anion radical should be more stable than the DEBMM anion radical, because the resonance structures of the EBPA anion radical could help further stabilize the negative charge. Therefore, EBPA should be more active in the photo-oxidation of EY, resulting in the faster quenching of EY. In contrast, the MBriB anion radical should be less stable than the DEBMM anion radical, because MBriB has less electron-withdrawing groups
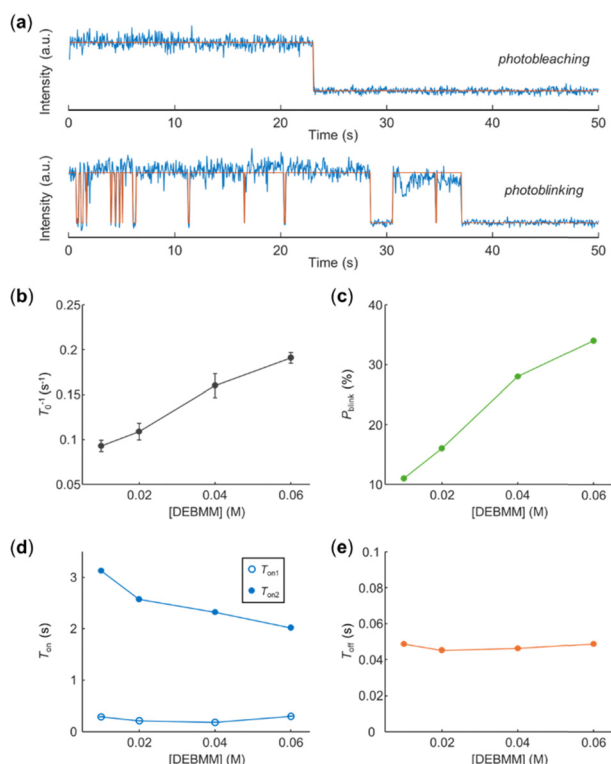

Fig. 2 (a) Photobleaching and photoblinking trajectories of single EYs in DEBMM. (b)–(e) The effect of DEBMM concentration on (b) photobleaching rate of EY T_0^{-1}, (c) percentage of photoblinking EY P_{blink}, (d) T_{on1} and T_{on2} of photoblinking EYs, and (e) T_{off} of photoblinking EYs.
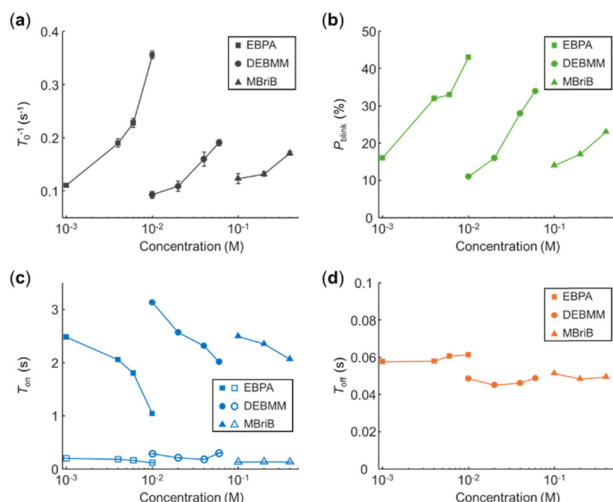
Fig. 3 The effect of alkyl bromide concentrations on (a) photobleaching rate of EY T_0^{-1}, (b) percentage of photoblinking EY P_{blink}, (c) T_{on1} (open symbols) and T_{on2} (filled symbols) of photoblinking EYs, and (d) T_{off} of photoblinking EYs.

than DEBMM. Therefore, MBriB should be less active in the photo-oxidation of EY, resulting in the slower quenching of EY. Like in DEBMM, the photoblinking on-time of EY (τ_{on}) followed double-exponential distributions in both EBPA and MBriB. The faster decay constants T_{on1} were nearly unaffected by EBPA and MBriB concentrations (Fig. 3c), and the slower decay constants T_{on2} decreased obviously with EBPA and MBriB concentrations (Fig. 3c). The decay constants of photoblinking off-time T_{off} remained nearly unchanged under various EBPA and MBriB concentrations (Fig. 3d). The results suggested that BET between $EY^{\bullet+}$ and alkyl bromide radical anions exists generally, and the BET probability could be related to the activity of alkyl bromide in PET.

In the end, we investigated the interaction between EY and tertiary amine. In the solution of TEA, the majority of EYs were photobleached in a single step. The photobleaching rate of EY (T_0^{-1}) increased with TEA concentration as expected (Fig. 4a). However, the percentage of photoblinking EY stayed at a very low level and did not increase with TEA concentration (Fig. 4b), which was different compared to the phenomena in alkyl bromides. This result indicated that there is no efficient BET between $EY^{\bullet-}$ and $TEA^{\bullet+}$.

The BET between $EY^{\bullet+}$ and alkyl bromide radical anions could explain the mechanism of EY-catalyzed photoinduced

atom transfer radical polymerization (photoATRP).[28] The reaction is proposed to follow a reductive quenching mechanism, in which EY* is first reduced by tertiary amine to $EY^{\bullet-}$ and then oxidized by alkyl bromide (ATRP initiator) to EY. The alkyl bromide radical anion then generates an alkyl radical to initiate polymerization. Based on the redox potentials,[23,29] EY* (either $^1EY^*$ or $^3EY^*$) can directly reduce alkyl bromide to an alkyl bromide radical anion to initiate polymerization. However, little polymer was produced without tertiary amine.[28,29] Based on our observations in this work, the reason is likely that the efficient BET between $EY^{\bullet+}$ and alkyl bromide radical anions significantly suppressed the generation of free radicals through the photoinduced electron transfer between EY* and alkyl bromides. Furthermore, the proposed reductive quenching mechanism is also supported by our observation that the BET efficiency between $EY^{\bullet-}$ and the tertiary amine radical cation is inefficient.

In summary, we investigated the interaction of commonly used quenchers with EY photoredox catalyst by single-molecule fluorescence imaging. In all quenchers, the photobleaching of EYs was accelerated, indicating the quenchers quenched EY *via* an electron transfer process. In alkyl bromide quenchers, large fractions of EYs showed photoblinking behavior, suggesting the existence of BET between $EY^{\bullet+}$ and alkyl bromide radical anions. In comparison, in tertiary amine TEA, the fraction of photoblinking EY was much lower, suggesting that there is no efficient BET between $EY^{\bullet-}$ and $TEA^{\bullet+}$. And the mechanism of EY-catalyzed photoATRP can be explained by the difference of quenchers in BET efficiency. In future, BET between other photo-emissive photoredox catalysts and redox quenchers can be studied by the single-molecule imaging method.

Data availability

The data supporting this article have been included as part of the ESI.†

Conflicts of interest

There are no conflicts to declare.

Notes and references

1 D. A. Nicewicz and D. W. C. MacMillan, *Science*, 2008, **322**, 77–80.
2 M. A. Ischay, M. E. Anzovino, J. Du and T. P. Yoon, *J. Am. Chem. Soc.*, 2008, **130**, 12886.
3 J. M. Narayanam, J. W. Tucker and C. R. Stephenson, *J. Am. Chem. Soc.*, 2009, **131**, 8756–8757.
4 D. P. Hari and B. König, *Org. Lett.*, 2011, **13**, 3852–3855.
5 C. K. Prier, D. A. Rankic and D. W. C. MacMillan, *Chem. Rev.*, 2013, **113**, 5322–5363.
6 D. P. Hari and B. Konig, *Chem. Commun.*, 2014, **50**, 6688–6699.
7 D. M. Arias-Rotondo and J. K. McCusker, *Chem. Soc. Rev.*, 2016, **45**, 5803–5820.
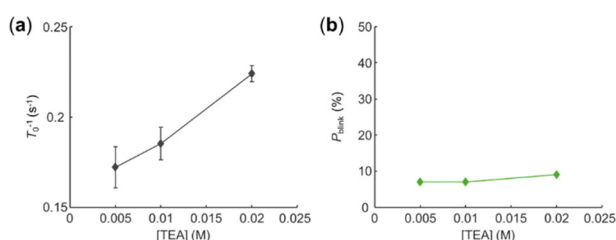8 L. Marzo, S. K. Pagire, O. Reiser and B. Konig, *Angew. Chem., Int. Ed.*, 2018, **57**, 10034–10072.

Fig. 4 The effect of TEA concentration on (a) photobleaching rate of EY T_0^{-1}, and (b) percentage of photoblinking EY P_{blink}.

9 Visible Light Photocatalysis in Organic Chemistry, Wiley-VCH Verlag GmbH & Co. KGaA, 2018.

10 G. J. Kavarnos and N. J. Turro, *Chem. Rev.*, 1986, **86**, 401–449.

11 J. Olmsted and T. J. Meyer, *J. Phys. Chem.*, 1987, **91**, 1649–1655.

12 M. Z. Hoffman, *J. Phys. Chem.*, 1988, **92**, 3458–3464.

13 A. I. Arkhypchuk, T. T. Tran, R. Charaf, L. Hammarström and S. Ott, *Inorg. Chem.*, 2023, **62**, 18391–18398.

14 H. Sayre, H. H. Ripberger, E. Odella, A. Zieleniewska, D. A. Heredia, G. Rumbles, G. D. Scholes, T. A. Moore, A. L. Moore and R. R. Knowles, *J. Am. Chem. Soc.*, 2021, **143**, 13034–13043.

15 A. Runemark and H. Sundén, *J. Org. Chem.*, 2023, **88**, 462–474.

16 B. P. Fors and C. J. Hawker, *Angew. Chem., Int. Ed.*, 2012, **51**, 8850–8853.

17 J. C. Theriot, C. H. Lim, H. Yang, M. D. Ryan, C. B. Musgrave and G. M. Miyake, *Science*, 2016, **352**, 1082–1086.

18 J. T. Xu, S. Shanmugam, H. T. Duong and C. Boyer, *Polym. Chem.*, 2015, **6**, 5615–5624.

19 C. Wang, H. Li, T. H. Bürgin and O. S. Wenger, *Nat. Chem.*, 2024, **16**, 1151–1159.

20 A. Ripak, S. De Kreijger, R. N. Sampaio, C. A. Vincent, E. Cauet, I. Jabin, U. K. Tambar, B. Elias and L. Troian-Gautier, *Chem Catal.*, 2023, 3.

21 A. Ripak, S. De Kreijger, B. Elias and L. Troian-Gautier, *STAR Protoc.*, 2023, **4**, 102312.

22 K. Gu, C. Yu, W. Zhou and C. Liu, *J. Phys. Chem. Lett.*, 2024, **15**, 717–724.

23 N. A. Romero and D. A. Nicewicz, *Chem. Rev.*, 2016, **116**, 10075–10166.

24 K. Gu, S. Liu and C. Liu, *Langmuir*, 2022, **38**, 15848–15857.

25 K. Gu and C. Liu, *Chem. Biomed. Imaging*, 2023, **1**, 234–241.

26 D. Fernandez Reina, A. Ruffoni, Y. S. S. Al-Faiyz, J. J. Douglas, N. S. Sheikh and D. Leonori, *ACS Catal.*, 2017, **7**, 4126–4130.

27 W. Tang and K. Matyjaszewski, *Macromolecules*, 2007, **40**, 1858–1863.

28 C. Kutahya, F. S. Aykac, G. Yilmaz and Y. Yagci, *Polym. Chem.*, 2016, **7**, 6094–6098.

29 C. Bian, Y. N. Zhou, J. K. Guo and Z. H. Luo, *Macromolecules*, 2018, **51**, 2367–2376.